


RESEARCH ARTICLE

Characterization of clot composition in acute cerebral infarct using machine learning techniques

Jong-Won Chung^{1,a} , Yoon-Chul Kim^{2,a}, Jihoon Cha³, Eun-Hyeok Choi¹, Byung Moon Kim³, Woo-Keun Seo¹, Gyeong-Moon Kim¹ & Oh Young Bang¹

¹Department of Neurology, Samsung Medical Center, Sungkyunkwan University School of Medicine, Seoul, Republic of Korea

²Clinical Research Institute, Samsung Medical Center, Sungkyunkwan University School of Medicine, Seoul, Republic of Korea

³Department of Radiology, Yonsei University Medical Center, Yonsei University College of Medicine, Seoul, Republic of Korea

Correspondence

Oh Young Bang, Department of Neurology, Samsung Medical Center, Sungkyunkwan University, 81, Irwon-Ro, Gangnam-gu, Seoul 06351, Republic of Korea. Tel: +82-2-3410-3599; Fax: +82-2-3410-0052; E-mail: ohyoung.bang@samsung.com

Funding Information

This study was supported by a grant from the Korean Health Technology R&D Project, the Ministry of Health & Welfare (HC15C1056), and the National Research Foundation of Korea (No. 2018R1A2B2003489).

Received: 3 October 2018; Revised: 31 January 2019; Accepted: 11 February 2019

Annals of Clinical and Translational Neurology 2019; 6(4): 739–747

doi: 10.1002/acn3.751

^aJ-W Chung and Y-C Kim contributed equally to this work.

Abstract

Objective: Clot characteristics can provide information on the cause of cerebral artery occlusion and may guide acute revascularization and secondary prevention strategies. We developed a rapid automated clot analysis system using machine learning (ML) and validated its accuracy in patients undergoing endovascular treatment. **Methods:** Pre-endovascular treatment gradient echo (GRE) images from consecutive patients with middle cerebral artery occlusion were utilized to develop and validate an ML system to predict whether atrial fibrillation (AF) was the underlying cause of ischemic stroke. The accuracy of the ML algorithm was compared with that of visual inspection by neuroimaging specialists for the presence of blooming artifact. Endovascular procedures and outcomes were compared in patients with and without AF. **Results:** Of 67 patients, 29 (43.3%) had AF. Of these, 13 had known AF and 16 were newly diagnosed with cardiac monitoring. By visual inspection, interrater correlation for blooming artifact was 0.73 and sensitivity and specificity for AF were 0.79 and 0.63, respectively. For AF classification, the ML algorithms yielded an average accuracy of > 75.4% in fivefold cross-validation with clot signal profiles obtained from 52 patients and an area under the curve >0.87 for the average AF probability from five signal profiles in external validation ($n = 15$). Analysis with an in-house interface took approximately 3 min per patient. Absence of AF was associated with increased number of passes by stentriever, high reocclusion frequency, and additional use of rescue stenting and/or glycogen IIb/IIIa blocker for recanalization. **Interpretation:** ML-based rapid clot analysis is feasible and can identify AF with high accuracy, enabling selection of endovascular treatment strategy.

Introduction

Neuroimaging in acute ischemic stroke plays an important role in selecting candidates for revascularization therapy based on the distribution and extent of infarct core, collateral, penumbra, and blood–brain barrier, and in determining the mode of treatment based on clot characteristics.¹ Identifying the characteristics of clots blocking brain vessels in acute ischemic stroke may provide important information in determining strategies of revascularization therapy as well as in choosing antithrombotics for secondary prevention of stroke.² Knowledge of clot characteristics may help predict the recanalization rate, time

required for re-opening, and optimal mode of treatment.³ In addition, the effects of antiplatelet agents and anticoagulants differ depending on the stroke subtype.⁴

As machine learning (ML), more specifically deep learning, shows remarkable performance in computer vision as well as in medical image analysis,⁵ it is increasingly being used in acute stroke neuroimaging.^{6,7} For example, segmentation of infarct core and penumbra with ML algorithms demonstrated high accuracy compared to experts' manual annotations or commercial software.^{8–10} The accurate identification of diffusion and perfusion lesions helps select patients eligible for endovascular treatment (EVT). The estimation of infarct core and

penumbra is related to the development of learning models in predicting final infarct distribution or patient outcome in cases of favorable and unfavorable responses to reperfusion therapy.^{11–13} Another ML application is the prediction of risks of hemorrhagic transformation from image data with blood–brain barrier information.¹⁴ The ML-based prediction of hemorrhagic transformation may serve as a decision support tool for reperfusion therapy. Finally, ML was applied to the task of selecting patients less than 4.5 hours from stroke onset.^{15,16} This may be particularly helpful in selecting patients with unknown onset to imaging time for intravenous thrombolysis.

Previous studies have indicated that vessel signs from noncontrast computed tomography (CT) and gradient-echo (GRE) magnetic resonance imaging (MRI) help elucidate clot composition in acute ischemic stroke.^{17–19} Hyperdense artery sign in CT or blooming artifact in MRI is associated with red blood cell (RBC)-rich clots.^{20,21} Image features such as two-layered susceptibility vessel sign (SVS), overestimation ratio, and SVS diameter have been demonstrated to be effective in predicting cardioembolic stroke.^{3,22,23} In the previous literature, two-layered SVS was assessed by visual inspection, and the quantification of overestimation ratio and SVS diameter relied on manual procedures by expert neurologists. The use of ML-based pattern recognition in clot characterization may be advantageous, since the decision making can be automated and the issue of intra and interrater variability can be alleviated.

This study investigated the feasibility of analyzing clot characteristics using GRE MRI and ML, with the expectation that ML could provide reliable assessment of clot characteristics. In addition, the clinical impact of ML-based MRI clot analysis on endovascular procedures and outcomes was considered in patients who received endovascular treatment.

Methods

Patients and work-ups

This study included patients who were admitted to a university medical center and underwent EVT between April 1, 2014 and February 31, 2017. The study inclusion criteria were as follows: (1) middle cerebral artery (MCA) occlusion, (2) MRI including gradient echo (GRE) sequence performed prior to EVT, and (3) EVT within 12 h of symptom onset. Patients with poor GRE image quality due to motion artifact were excluded.

Demographic information, history of vascular risk factors, and initial National Institutes of Health Stroke Scale (NIHSS) scores were systematically collected. Radiologic information (time interval from symptom onset to MRI) and stroke treatment information (intravenous tissue

plasminogen activator, onset to initiation of EVT, and duration of EVT) were obtained by reviewing electronic medical records. We performed standard cardiac source evaluation, including multiple electrocardiograms, transthoracic or transesophageal echocardiography, 24-h Holter monitoring, and cardiac telemetry (72 h or more).²⁴ Local institutional review boards approved this study. All participants or patient guardians provided informed consent.

Visual inspection of blooming artifact

Based on visual inspection, the presence or absence of blooming artifact was scored by two neuroimaging experts, who were experienced in stroke MRI reading and blinded to clinical information. For each subject's data, each rater navigates the axial slices and identifies a slice showing MCA. When MCA was captured in more than one slice, the slice with larger MCA was chosen for scoring. Blooming artifact was defined as an area of hypointensity or signal loss in the proximal MCA, distorting the margins of the vessel with enlargement of vessel contour. The raters re-scored presence of blooming artifact 2 weeks later to estimate interobserver variability. The interrater agreement for the measurement of blooming artifact was assessed using the Kappa statistics and 95% confidence interval. The results of visual inspection and presence of atrial fibrillation were analyzed.

Region of interest allocation and extraction of signal graphic information

MRI data were acquired on a 3T scanner system (Philips Achieva, Best, The Netherlands) using a gradient-echo (GRE) sequence with slice thickness = 5 mm, interslice gap = 1.5 mm, TR = 610 msec, TE = 16 msec, flip angle = 18°, field of view = 240 mm, acquisition matrix size = 256 × 249, and reconstruction matrix size = 560 × 560. The GRE images were normalized to [0, 1] to reduce the effect of the image intensity variability in the subjects. Figure 1D and E shows our in-house graphical user interface (GUI) developed in MATLAB (Mathworks, Natick, MA, USA). Procedures for GUI usage are described as follows. For each subject's data, a user navigates the axial slices and identifies a region of interest (ROI) indicating blooming artifact in the MCA. When MCA was captured in more than one slice, the slice with larger MCA was chosen for evaluation. The start and end points are clicked by the user; then, a centerline connecting the two points is drawn and covers the clot ROI automatically. When the start and end points are determined, 30-pixel-wide lines are drawn to be parallel to each other and perpendicular to the centerline. A line profile plot is obtained from the

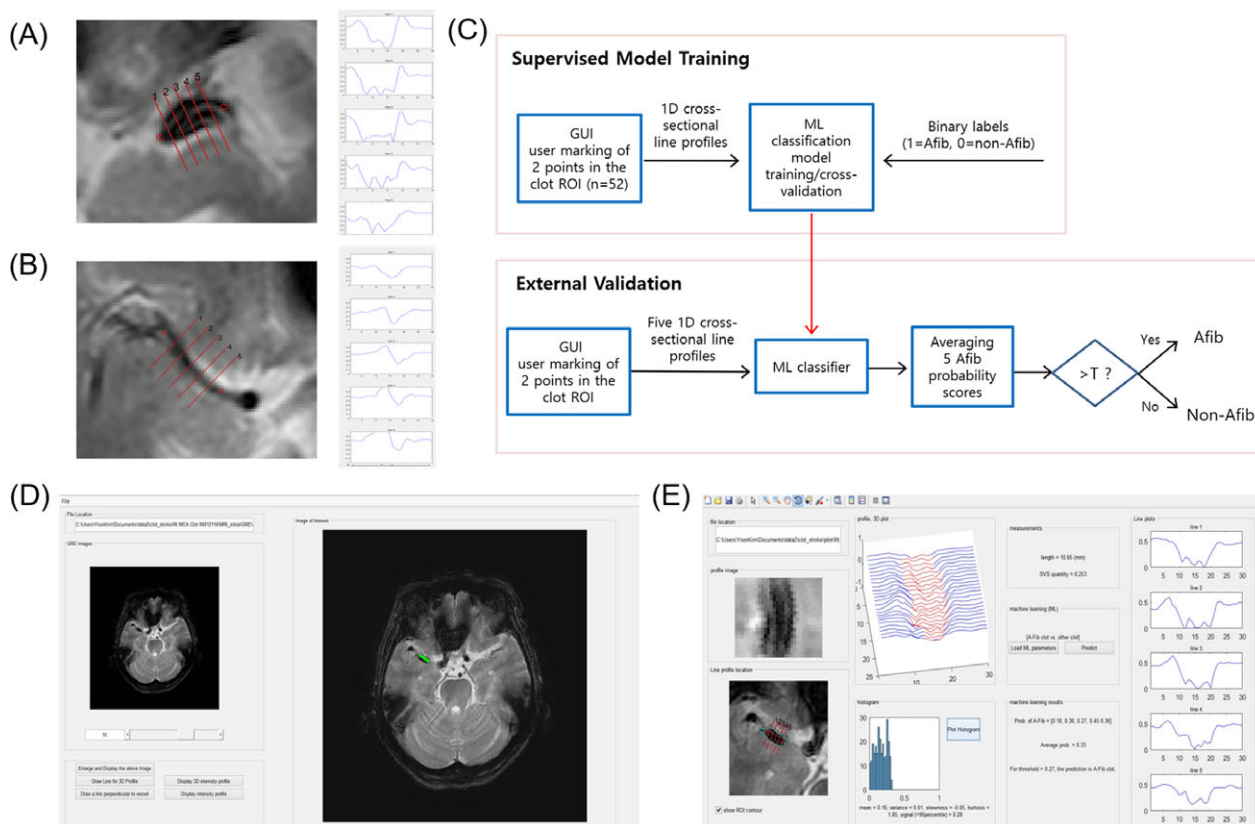


Figure 1. Basic scheme of machine learning-based clot analysis. (A, B) The red circles indicate user-marked start and end points of clot ROI. The five red lines were located vertical to user-marked clot location at even intervals and were used to extract signal intensities for graphic analysis. (A, Clot related to atrial fibrillation; B, Clot unrelated to atrial fibrillation). (C) Flowchart of the proposed ML-based clot characterization method, where T is the threshold for Afib/non-Afib classification. (D, E) Custom GUI for clot analysis. ROI, region of interest; GUI, graphical user interface; Afib, atrial fibrillation; ML, machine learning; T, threshold.

intensity values on each line. Each line profile served as feature input to a machine learning classifier model. Figure 1 shows representative ROI images and associated intensity profiles for clot in patients with atrial fibrillation (Fig. 1A) and without atrial fibrillation (Fig. 1B). The procedures were semiautomatic and took approximately 3 min per patient from loading of the GRE DICOM images in the GUI until machine learning prediction of the AF clot characteristics.

Development of supervised machine learning model

Step 1. Model development

For ML model, individual patient's GRE images were included. The model did not include any clinical data in order for the model to be performed without any additional manual entering of variables. Training data were obtained from 52 subjects ($n = 22$ for atrial fibrillation, $n = 30$ for nonatrial fibrillation). For each subject, samples of the number of line profiles \times 30 vectors were obtained

after specification of the start and end points in a clot ROI. We augmented the number of samples twice by horizontally flipping each intensity profile. The dimensions of ($\#$ of samples) \times ($\#$ of features) in the training dataset were 2048×30 , which was the input to the ML model. The 2048 samples consisted of 920 AF samples and 1128 non-AF samples. Figure 1C displays the flow chart of our ML-based clot characterization framework. For comparison, we tested random forests, support vector machine, artificial neural network, and logistic regression algorithms since these four models have distinct characteristics in model training and are widely used for classification.²⁵

Step 2. Model validation

With the training dataset, fivefold cross-validation was performed to evaluate the performance of the four ML models. The cross-validation folds were constructed based on the patient, rather than based on the intensity profile. The fold 1, 2, and 3 each contained the intensity profiles from 4 AF and 6 non-AF patients, whereas the fold 4 and

5 each had the intensity profiles from 5 AF and 6 non-AF patients. The assignment of the patients to each fold was performed in a random manner. The ML models of random forests, support vector machine, artificial neural network, and logistic regression, provided by the Python's scikit-learn package were used for cross-validation.²⁶ After hyperparameter selection of each model using grid search, mean and standard deviation of the cross-validation accuracy were computed for each model.

For external validation, we used GRE images from 15 unseen subjects, who arrived at the hospital in the later period ($n = 7$ for atrial fibrillation, $n = 8$ for nonatrial fibrillation), and tested the performance of the binary classification of clot characteristics. The GRE image protocol and clinical evaluation methods for detection of atrial fibrillation in the development and validation groups were identical in this study. For each subject, users identified the clot ROI and clicked the start and end points. Five perpendicular line profiles were automatically drawn as shown in Figure 1E. There are other choices in the number of line profiles, but empirically 5 per clot ROI was the reasonable number of line profiles based on the lengths of visually evident clots in all the subjects considered. Each line profile was fed to the trained ML model. A probability of AF clot was obtained as a result of the classifier, except for the support vector machine which produced binary values 0 or 1 as output. For the clot ROI of interest, final average atrial fibrillation probability ($P_{AF,avg}$) was obtained after averaging of the five predicted AF probabilities. A receiver operating characteristic (ROC) curve was plotted to evaluate the model's prediction performance at various settings of the $P_{AF,avg}$ thresholds. In the clot analysis GUI, the threshold "T" in Figure 1C was determined to meet a proper trade-off between sensitivity and specificity. The value of threshold "T" in the GUI can be used for binary decision of AF/non-AF.

Statistical analysis

Descriptive demographics and clinical and radiological data are shown as mean \pm standard deviations or numbers and frequencies, as appropriate. We analyzed the differences among the groups using chi-square or Mann-Whitney tests for discrete variables and one-way analysis of variance or Kruskal-Wallis tests for continuous variables. Sensitivity and specificity were compared in between visual inspection and machine learning-based clot analysis for underlying atrial fibrillation.

Results

Of 129 consecutive patients treated with EVT during the study period, 81 were diagnosed with stroke caused by an

MCA occlusion. After excluding 10 patients who did not have GRE MRI prior to EVT or whose GRE image quality was inadequate for analysis, and 4 with no visible MCA on GRE imaging, a total of 67 were included in the final analysis. Among these 67 eligible patients, 41 (61.2%) were male, with a mean age of 61.7 ± 16.2 years, and 29 (43.3%) had atrial fibrillation; of these, 13 (44.8%) had known atrial fibrillation and 16 (55.2%) were newly diagnosed with prolonged cardiac monitoring. Median onset to GRE imaging time was 120 min (interquartile range, 99–185), and median onset to groin puncture was 183 min (interquartile range, 146–230). Comparisons of demographic, clinical, laboratory, and treatment profiles of the study subjects according to the absence or presence of atrial fibrillation are summarized in Table 1. Inter and intrarater agreement for blooming artifact was poor; (1) Interrater agreement Kappa, 0.73; 95% confidence interval, 0.60–0.83, (2) Intrarater agreement #1 agreement Kappa, 0.70; 95% confidence interval, 0.47–0.94, (3) Intrarater agreement #1 agreement Kappa, 0.73; 95% confidence interval, 0.65–0.88.

The discordant cases were re-reviewed and final blooming artifact was determined by consensus. The sensitivity and specificity for underlying atrial fibrillation were 0.79 and 0.63, respectively (area under the curve, 0.78). For the ML classification techniques, the fivefold cross-validation resulted in mean accuracy (standard deviation) of 75.4 (± 7.7) % for random forest, 78.7 (± 9.4) % for support vector machine, 75.5 (± 10.4) % for artificial neural network, and 77.3 (± 9.4) % for logistic regression, respectively. The external validation resulted in the areas under the curve of 0.87–0.93 and 0.91–0.93 for observer 1 and observer 2, respectively (Fig. 2).

Among the 67 patients, 55 (82.1%) were treated with stentriever-based endovascular procedures. Compared to patients with atrial fibrillation, more retrieval passes (3 [3–4] vs. 2 [1–3], $P < 0.001$) and more frequent reocclusion (2 [0–4] vs. 0 [0–0], $P < 0.001$) were observed in patients without atrial fibrillation. Using a stentriever, successful recanalization (modified Treatment in Cerebral Infarction $\geq 2b$) was achieved in 2 (7.9%) patients without atrial fibrillation and 19 (65.5%) with atrial fibrillation ($P < 0.001$). Additional recanalization was achieved with MCA stenting or intraarterial glycogen IIb/IIIa blocker infusion in 13 (34.2%) patients without atrial fibrillation and 2 (3.8%) with atrial fibrillation. The details of EVT according to clot characteristics are summarized in Table 2. Representative cases of clot analysis in atrial fibrillation and intracranial atherosclerotic occlusion are presented in Figure 3.

Discussion

The major findings of this study were as follows. In patient with acute MCA occlusion, pretreatment GRE

Table 1. Baseline characteristics according to presence of atrial fibrillation.

	Without atrial fibrillation (<i>n</i> = 38)	With atrial fibrillation (<i>n</i> = 29)	<i>P</i> -value
Age (year), mean ± SD	56.5 ± 17.8	68.4 ± 10.8	0.002
Male sex, <i>n</i> (%)	26 (68.4)	15 (51.7)	0.165
Hypertension, <i>n</i> (%)	19 (50.0)	15 (51.4)	0.889
Diabetes, <i>n</i> (%)	7 (18.4)	8 (27.6)	0.373
Dyslipidemia, <i>n</i> (%)	5 (13.2)	6 (20.7)	0.41
Atrial fibrillation, <i>n</i> (%)			NA
Previously diagnosed	0 (0.0)	13 (44.8)	
Newly detected	0 (0.0)	16 (55.2)	
Other causes of clot			NA
Intracranial atherosclerosis	24 (63.2)	0 (0.0)	
Thromboembolism from carotid plaque	6 (15.8)	0 (0.0)	
Other and undetermined sources ¹	8 (21.0)	0 (0.0)	
Initial NIHSS score	12 [9–16]	15 [12–18]	0.038
Intravenous tPA, <i>n</i> (%)	23 (60.5)	22 (75.9)	0.185
Glucose (mg/mL), mean ± SD	133.2 ± 42.7	118.0 ± 20.7	0.083
Systolic blood pressure (mmHg), mean ± SD	139.7 ± 21.6	140.9 ± 17.6	0.814
Symptom to ER arrival, median (IQR)	53 [28–98]	45 [31–123]	0.537
Symptom to GRE imaging, median (IQR)	124 [94–183]	116 [101–187]	0.368
Symptom to groin puncture (min), median (IQR)	190 [145–227]	180 [157–240]	0.502

SD, standard deviation; tPA, NIHSS, National Institutes of Health stroke scale; Tissue plasminogen activator; ER, emergency room; IQR, interquartile range; GRE, gradient echo.

¹Paradoxical embolism in 2, aortic arch atheroma in 1, and undetermined source in 5.

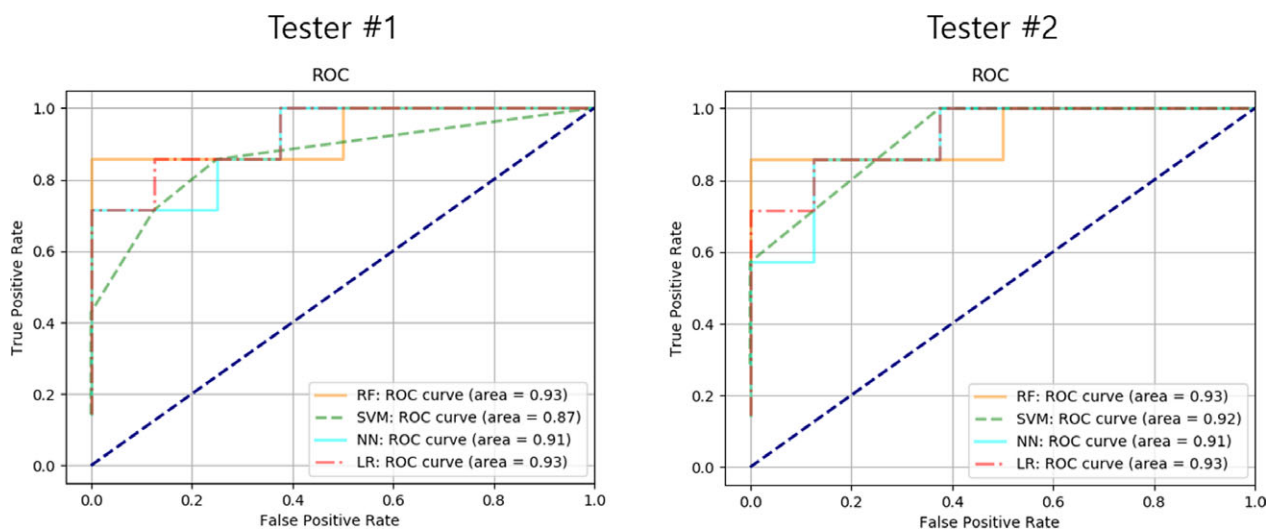


Figure 2. ROC curves for external validation (*n* = 15) in classification of AF and non-AF clots. For each patient, two testers blinded to clinical information evaluated the classification of AF and non-AF clots in the custom GUI, by taking the five intensity profiles in a clot ROI as input to four different machine learning classifiers. ROC, receiver operating characteristic; RF, random forests; SVM, support vector machine; NN, neural network; LR, logistic regression.

image-based clot analysis was feasible, and a machine learning-based clot analysis algorithm predicted atrial fibrillation with high accuracy. Response to EVT and the need for therapy differed between patients with and without atrial fibrillation as well as according to the characteristics of clot imaging. This suggests that utilization of a

machine learning algorithm for evaluation of clot characteristics based on GRE imaging could be helpful in selecting an appropriate EVT modality and may lead to faster recanalization in patients with MCA occlusion.

There have been efforts to visualize the clot in patients with acute ischemic stroke. Clot characteristics can be

Table 2. Endovascular treatment procedures and outcome by presence of atrial fibrillation.

	Without atrial fibrillation (n = 38)	With atrial fibrillation (n = 29)	P-value
Intravenous tPA before procedure, n (%)	23 (60.5)	22 (75.9)	0.185
Treatment modality, n (%)			
Stentriever	31 (81.6)	24 (82.8)	0.901
Stent	7 (18.4)	1 (3.4)	0.061
Glycogen IIb/IIIa blocker	11 (28.9)	2 (6.9)	0.024
Procedural event, median [IQR]			
Number of retrieval passes	3 [3–4]	2 [1–3]	<0.001
Number of reocclusions during procedure	2 [0–4]	0 [0–0]	<0.001
Total procedure time (min)	101.6 ± 46.1	82.4 ± 36.4	0.07
Procedural outcomes, n (%)			
mTICI 2b or 3 by stentriever	16 (42.1)	21 (72.4)	0.013
by other modality	3 (7.9)	19 (65.5)	<0.001
Stent	7 (18.4)	1 (3.4)	0.061
Glycogen IIb/IIIa blocker	6 (15.8)	1 (3.4)	0.102

tPA, Tissue plasminogen activator; IQR, interquartile range; mTICI, modified Treatment in Cerebral Infarction.

expressed by the length/burden and composition, which may be related to etiopathologic subtypes of stroke. The importance of clot burden in intravenous thrombolysis has been evaluated with computed tomography (CT) and MR angiography.^{27–29} Recent studies attempted to measure clot burden using clot volume and length with non-contrast CT or CT angiography. However, conflicting results have been reported for the association with successful endovascular recanalization,³⁰ and results from recent randomized clinical trials showed that clot burden score did not modify the effects of EVT.^{31,32} In addition, thin (e.g., 1 mm) scan thickness and software for post-processing was required to measure clot volume and length using CT images, which may not be practical in the setting of EVT for acute ischemic stroke. In addition, successful reperfusion could be associated with the histopathology of occlusive thrombi, including the existence of atheromatous gruel and proportion of erythrocyte components.³³ Although there have been efforts to predict the response to revascularization therapy using CT clot imaging, a recent systematic analysis showed a lack of association between CT-based clot image (e.g., Hounsfield units) and the histopathology of thrombi or stroke etiology.²⁰

MRI can identify clot with high specificity and can measure clot burden more clearly than CT images.^{34–36} Blooming artifact, caused by paramagnetic materials, in GRE or susceptible weighted images has been associated

with cardioembolic stroke.^{3,23} Compared to large artery atherosclerosis, clot with atheromatous plaque, deoxyhemoglobin, and hemosiderin in the erythrocyte can cause a paramagnetic blooming effect. In a pathology study with thrombi retrieved via EVT, blooming artifact appearance was determined by the presence of red blood cells, and their absence indicated fibrin-predominant occlusive thrombi.¹⁷ The limitation of brain MRI including GRE imaging requires longer scan time compared to CT. Although a comprehensive MRI protocol can be performed in 20 min, a fast MRI protocol can be performed in 6 min, rivaling that of any comprehensive acute stroke CT protocol.³⁷ This fast MRI protocol includes diffusion weighted imaging, fluid attenuated inversion recovery, GRE, MR angiography, and MR perfusion. We used a modified protocol that required a 9-min scanning time in candidates for EVT.³⁸ An additional 3 min were required for postprocessing and machine learning-based etiologic prediction of clot with GRE imaging. The 12-min protocol might be acceptable considering that decision making with trial-and-error for stentriever failure often requires tens of minutes or even hours.

Machine learning technique may help to increase inter-rater reliability in interpreting stroke imaging data. For example, Alberta Stroke Program Early CT score (e-ASPECT) software automatically generates a score from brain CT, and proved to be effective with a high degree of reliability in calculating the score compared to that calculated by a stroke physician and neuroradiologist.^{39,40} This study showed that compared to simple visual analysis of blooming effect by neuroimaging experts, machine learning technique increased interrater reliability, and overall reliability in terms of predicting atrial fibrillation with clot analysis. The advantages of machine learning technique over simple visual inspection include the extraction of various imaging features and analysis of large amounts of quantitative imaging data (“radiomics”). Utilization of machine learning technique with multimodal imaging including high-resolution MRI could be helpful in various stroke pathophysiologies. However, it should be noted that machine learning may be prone to misclassification errors in the case that some patients’ images are degraded by motion. In this study, we excluded a few patients whose GRE images were inadequate for analysis.

Stroke subtypes and related clot composition may determine the response to recanalization therapy.^{33,41,42} Although cardioembolic stroke, especially in association with atrial fibrillation, is the most common subtype in patients with acute disabling ischemic stroke, patients with other subtypes could be candidates for EVT. Intracranial atherosclerosis is especially prevalent in Asians and is associated with frequent EVT failure. In this

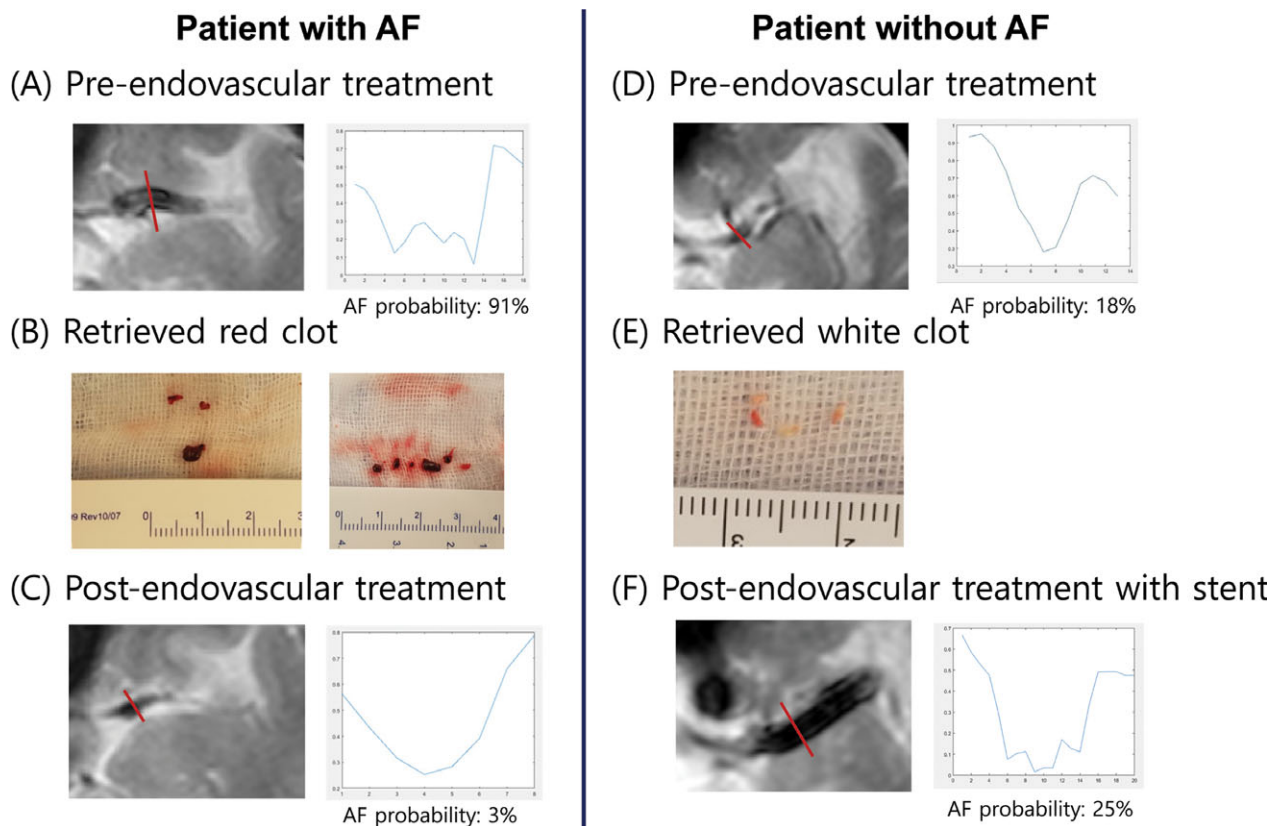


Figure 3. Representative cases of GRE vessel signal change after successful endovascular clot retrieval in atrial fibrillation and intracranial atherosclerosis patients. (A) Clot signal analysis prior to endovascular thrombectomy showing “W” shaped signal intensity. (B) Retrieved red clots. (C) Resolved “W” signal after successful removal of atrial fibrillation-related clot. (D) Clot signal analysis prior to endovascular thrombectomy showing “non-W”-shaped signal intensity. (E) Retrieved white clots. (F) Heterogeneous dark signal after successful recanalization of atherosclerotic occlusion with emergency stenting. GRE, gradient echo.

condition, adjuvant therapy, such as the use of a glycoprotein IIb/IIIa inhibitor or rescue stent placement, may be needed.^{43,44} Therefore, differentiation between intracranial atherosclerotic and cardiogenic embolic occlusion using pretreatment imaging data could help customize EVT.² In this study, the rate of successful recanalization with stentriever was lower in patients without atrial fibrillation and additional recanalization was achieved using rescue stenting and glycoprotein IIb/IIIa blocker treatment. In addition, there were more retrieval passes and reocclusion episodes and longer total procedure time in patients without atrial fibrillation. Therefore, etiologic diagnosis of arterial occlusion prior to EVT could be helpful in guiding EVT strategies.

Study limitations

This study has several limitations. First, this was a single-center study performed on a 3T scanner and a relatively small number of patients were available for analysis. In

addition, only Korean patients were included for analyses. Therefore, generalizability of the study findings may be limited. Given that we used routine MRI data, our method can be applied in the acute clinical setting, and our results should prompt larger, multicenter, multiethnicity, confirmatory studies. Furthermore, GRE image utilized in the study was not three-dimensional scans. Future study with three-dimensional GRE image could address partial volume effects with higher signal to noise ratio. Second, clinicians would determine presence of blooming artifact for standard of care, but neuroimaging experts scored blooming artifact in this study. However, this issue does not affect robustness of the study findings. Third, even though MCA occlusion is the most common reason for EVT, only MCA clots were analyzed and distal internal carotid artery, MCA branch, and basilar artery occlusions were excluded in this study. Further study is needed to evaluate and validate the study findings in other intracranial arteries. Fourth, GRE imaging used in the present study was performed with 5-mm section

thickness and interslice gap of 1.5 mm and was prone to a partial volume effect. Therefore, precise quantitative measurement of clot volume was not possible. Fifth, the study finding was not confirmed with pathologic evaluation. A prospective study with thrombus collection and pathologic correlation is warranted to confirm that machine learning-based noninvasive imaging analysis could determine thrombus composition. However, analysis of retrieved clot might not be the gold standard for clot characterization, given the conflicting results for the association between stroke subtype and histopathologic data.^{18,45,46} Finally, due to the retrospective nature of the study, we could not confirm whether EVT strategy selection based on clot characteristics could reduce procedure time and increase the rate of successful recanalization. Future study with a prospective design is warranted to evaluate angiographic and clinical outcomes of clot character-based EVT.

Conclusion

Our data indicate that machine learning-based rapid and noninvasive evaluation of clot characteristics is feasible and could provide information on clot composition in acute MCA occlusion patients. Further studies using multimodal MRI and machine learning-based evaluation of other stroke pathophysiologic factors, for example, collateral circulation, blood–brain barrier, and tissue perfusion status, and their association with EVT outcomes are warranted.

Acknowledgments

This study was supported by a grant from the Korean Health Technology R&D Project, the Ministry of Health & Welfare (HC15C1056), and the National Research Foundation of Korea (No. 2018R1A2B2003489).

Conflict of Interest

All authors declare that they have no conflict of interest.

References

- Bang OY, Chung JW, Son JP, et al. Multimodal MRI-based triage for acute stroke therapy: challenges and progress. *Front Neurol* 2018;9:586.
- Kim BM. Causes and solutions of endovascular treatment failure. *J Stroke* 2017;19:131–142.
- Kang DW, Jeong HG, Kim DY, et al. Prediction of stroke subtype and recanalization using susceptibility vessel sign on susceptibility-weighted magnetic resonance imaging. *Stroke* 2017;48:1554–1559.
- Powers WJ, Rabinstein AA, Ackerson T, et al. 2018 Guidelines for the early management of patients with acute ischemic stroke: a guideline for healthcare professionals from the American Heart Association/American Stroke Association. *Stroke* 2018;49:e46–e110.
- Litjens G, Kooi T, Bejnordi BE, et al. A survey on deep learning in medical image analysis. *Med Image Anal* 2017;42:60–88.
- Lee EJ, Kim YH, Kim N, Kang DW. Deep into the brain: artificial intelligence in stroke imaging. *J Stroke* 2017;19:277–285.
- Kamal H, Lopez V, Sheth SA. Machine learning in acute ischemic stroke neuroimaging. *Front Neurol* 2018;9:945.
- Chen L, Bentley P, Rueckert D. Fully automatic acute ischemic lesion segmentation in DWI using convolutional neural networks. *Neuroimage Clin* 2017;15:633–643.
- Zhang R, Zhao L, Lou W, et al. Automatic segmentation of acute ischemic stroke from DWI Using 3-D fully convolutional densenets. *IEEE Trans Med Imaging* 2018;37:2149–2160.
- McKinley R, Hung F, Wiest R, et al. A machine learning approach to perfusion imaging with dynamic susceptibility contrast MR. *Front Neurol* 2018;9:717.
- McKinley R, Hani L, Gralla J, et al. Fully automated stroke tissue estimation using random forest classifiers (FASTER). *J Cerebral Blood Flow Metab* 2017;37:2728–2741.
- Nielsen A, Hansen MB, Tietze A, Mouridsen K. Prediction of tissue outcome and assessment of treatment effect in acute ischemic stroke using deep learning. *Stroke* 2018;49:1394–1401.
- Pinto A, McKinley R, Alves V, et al. Stroke lesion outcome prediction based on MRI imaging combined with clinical information. *Front Neurol* 2018;9:1060.
- Yu Y, Guo D, Lou M, et al. Prediction of hemorrhagic transformation severity in acute stroke from source perfusion MRI. *IEEE Trans Bio-Med Eng* 2018;65:2058–2065.
- Ho KC, Speier W, El-Saden S, Arnold CW. Classifying acute ischemic stroke onset time using deep imaging features. *AMIA Annu Symp Proc* 2017;2017:892–901.
- Wouters A, Cheng B, Christensen S, et al. Automated DWI analysis can identify patients within the thrombolysis time window of 4.5 hours. *Neurology* 2018;90:e1570–e1577.
- Liebeskind DS, Sanossian N, Yong WH, et al. CT and MRI early vessel signs reflect clot composition in acute stroke. *Stroke* 2011;42:1237–1243.
- Kim SK, Yoon W, Kim TS, et al. Histologic analysis of retrieved clots in acute ischemic stroke: correlation with stroke etiology and gradient-Echo MRI. *AJNR Am J Neuroradiol* 2015;36:1756–1762.
- Simons N, Mitchell P, Dowling R, et al. Thrombus composition in acute ischemic stroke: a histopathological

- study of thrombus extracted by endovascular retrieval. *J Neuroradiol* 2015;42:86–92.
20. Brinjikji W, Duffy S, Burrows A, et al. Correlation of imaging and histopathology of thrombi in acute ischemic stroke with etiology and outcome: a systematic review. *J Neurointerv Surg* 2017;9:529–534.
 21. Cho KH, Kim JS, Kwon SU, et al. Significance of susceptibility vessel sign on T2*-weighted gradient echo imaging for identification of stroke subtypes. *Stroke* 2005;36:2379–2383.
 22. Yamamoto N, Satomi J, Tada Y, et al. Two-layered susceptibility vessel sign on 3-tesla T2*-weighted imaging is a predictive biomarker of stroke subtype. *Stroke* 2015;46:269–271.
 23. Zhang R, Zhou Y, Liu C, et al. Overestimation of susceptibility vessel sign: a predictive marker of stroke cause. *Stroke* 2017;48:1993–1996.
 24. Saver JL. Clinical practice. Cryptogenic Stroke. *N Engl J Med* 2016;374:2065–2074.
 25. van Os HJA, Ramos LA, Hilbert A, et al. Predicting outcome of endovascular treatment for acute ischemic stroke: potential value of machine learning algorithms. *Front Neurol* 2018;9:784.
 26. Pedregosa F, Varoquaux G, Gramfort A, et al. Scikit-learn: machine learning in Python. *J Mach Learn Res.* 2011;12 (Oct):2825–2830.
 27. Behrens L, Mohlenbruch M, Stampfl S, et al. Effect of thrombus size on recanalization by bridging intravenous thrombolysis. *Eur J Neurol* 2014;21:1406–1410.
 28. Strbian D, Sairanen T, Silvennoinen H, et al. Intravenous thrombolysis of basilar artery occlusion: thrombus length versus recanalization success. *Stroke* 2014;45:1733–1738.
 29. Rohan V, Baxa J, Tupy R, et al. Length of occlusion predicts recanalization and outcome after intravenous thrombolysis in middle cerebral artery stroke. *Stroke* 2014;45:2010–2017.
 30. Heo JH, Kim K, Yoo J, et al. Computed tomography-based thrombus imaging for the prediction of recanalization after reperfusion therapy in stroke. *J Stroke* 2017;19:40–49.
 31. Mokin M, Levy EI, Siddiqui AH, et al. Association of clot burden score with radiographic and clinical outcomes following Solitaire stent retriever thrombectomy: analysis of the SWIFT PRIME trial. *J Neurointerv Surg* 2017;9:929–932.
 32. Treurniet KM, Yoo AJ, Berkhemer OA, et al. Clot burden score on baseline computerized tomographic angiography and intra-arterial treatment effect in acute ischemic stroke. *Stroke* 2016;47:2972–2978.
 33. Hashimoto T, Hayakawa M, Funatsu N, et al. Histopathologic analysis of retrieved thrombi associated with successful reperfusion after acute stroke thrombectomy. *Stroke* 2016;47:3035–3037.
 34. Park MG, Oh SJ, Baik SK, et al. Susceptibility-weighted imaging for detection of thrombus in acute cardioembolic stroke. *J Stroke* 2016;18:73–79.
 35. Naggara O, Raymond J, Domingo Ayllon M, et al. T2* “susceptibility vessel sign” demonstrates clot location and length in acute ischemic stroke. *PLoS ONE* 2013;8:e76727.
 36. Soize S, Batista AL, Rodriguez Regent C, et al. Susceptibility vessel sign on T2* magnetic resonance imaging and recanalization results of mechanical thrombectomy with stent retrievers: a multicentre cohort study. *Eur J Neurol* 2015;22:967–972.
 37. Nael K, Khan R, Choudhary G, et al. Six-minute magnetic resonance imaging protocol for evaluation of acute ischemic stroke: pushing the boundaries. *Stroke* 2014;45:1985–1991.
 38. Son JP, Lee MJ, Kim SJ, et al. Impact of slow blood filling via collaterals on infarct growth: comparison of mismatch and collateral status. *J Stroke* 2017;19:88–96.
 39. Herweh C, Ringleb PA, Rauch G, et al. Performance of e-ASPECTS software in comparison to that of stroke physicians on assessing CT scans of acute ischemic stroke patients. *Int J Stroke* 2016;11:438–445.
 40. Nagel S, Sinha D, Day D, et al. e-ASPECTS software is non-inferior to neuroradiologists in applying the ASPECT score to computed tomography scans of acute ischemic stroke patients. *Int J Stroke* 2017;12:615–622.
 41. Choi MH, Park GH, Lee JS, et al. Erythrocyte fraction within retrieved thrombi contributes to thrombolytic response in acute ischemic stroke. *Stroke* 2018;49:652–659.
 42. Laridan E, Denorme F, Desender L, et al. Neutrophil extracellular traps in ischemic stroke thrombi. *Ann Neurol* 2017;82:223–232.
 43. Baek JH, Kim BM, Kim DJ, et al. Importance of truncal-type occlusion in stentriever-based thrombectomy for acute stroke. *Neurology* 2016;87:1542–1550.
 44. Chang Y, Kim B, Bang O, et al. Rescue stenting for failed mechanical thrombectomy in acute ischemic stroke. *Stroke* 2018;49:958–964.
 45. Marder VJ, Chute DJ, Starkman S, et al. Analysis of thrombi retrieved from cerebral arteries of patients with acute ischemic stroke. *Stroke* 2006;37:2086–2093.
 46. Sporns PB, Hanning U, Schwandt W, et al. Ischemic stroke: what does the histological composition tell us about the origin of the thrombus? *Stroke* 2017;48:2206–2210.